

# High contrast internal and external coronagraph masks produced by various techniques

Kunjithapatham Balasubramanian\*, Daniel Wilson, Victor White, Richard Muller, Matthew Dickie, Karl Yee, Ronald Ruiz, Stuart Shaklan, Eric Cady, Brian Kern, Ruslan Belikov<sup>1</sup>, and Olivier Guyon<sup>2</sup>, N. Jeremy Kasdin<sup>3</sup>

Jet Propulsion Laboratory, California Institute of Technology  
4800 Oak Grove drive, Pasadena, CA 91109

<sup>1</sup>NASA Ames Research Center, Moffett Field, CA

<sup>2</sup>University of Arizona, Tucson, AZ; <sup>3</sup>Princeton University, NJ  
[kbala@jpl.nasa.gov](mailto:kbala@jpl.nasa.gov) Tel: 818-393-0258

## ABSTRACT

Masks for high contrast internal and external coronagraphic imaging require a variety of masks depending on different architectures to suppress star light. Various fabrication technologies are required to address a wide range of needs including gradient amplitude transmission, tunable phase profiles, ultra-low reflectivity, precise small scale features, and low-chromaticity. We present the approaches employed at JPL to produce pupil plane and image plane coronagraph masks, and lab-scale external occulter type masks by various techniques including electron beam, ion beam, deep reactive ion etching, and black silicon technologies with illustrative examples of each. Further development is in progress to produce circular masks of various kinds for obscured aperture telescopes.

**Keywords:** Exoplanet, coronagraph, mask, occulter, PIAA, Shaped pupil

## 1. INTRODUCTION

Detection and characterization of faint exoplanets require an efficient coronagraph to suppress the star light and allow planet light to get through to the final image plane of the telescope. Various coronagraph architectures are being studied for this purpose. Central to all coronagraphs are star light suppressing masks to function either in the focal plane or pupil plane or both. Modified Band Limited Coronagraph (BLC, Trauger<sup>1,2</sup>), Shaped Pupil Coronagraph (SPC, Belikov<sup>3</sup>), Vector Vortex Coronagraph (VVC, Mawet<sup>4</sup>), and Phase Induced Amplitude Apodization Complex Mask Coronagraph (PIAACMC, Guyon<sup>5,21</sup>) are chief among these architectures. Different kinds of masks are needed for each of these architectures and hence different technologies are needed to produce them. In addition, with the availability of the 2.4 m Astrophysics Focused Telescope Assets (AFTA) to NASA, the need has arisen for advanced coronagraphs that function with an obscured aperture. This further stresses the importance of high-quality circularly symmetric masks with accurate amplitude and phase profiles to perform apodization and achromatization at high levels of contrast for exoplanet detection. We present here illustrative examples of masks produced by various techniques at JPL.

## 2. BACKGROUND AND CURRENT EXPERIENCE

Two major categories of masks are needed for different types of coronagraph architectures: (1) achromatic focal plane mask, and (2) reflective or transmissive binary apodizers and pupil plane masks. To fabricate such masks, different complementary techniques have been explored at JPL for development and advancement: (1) electron beam evaporation through a scanning slit, (2) electron beam lithography, (3) deep reactive ion etching, (4) focused ion beam deposition, and (5) cryogenic black silicon processing.

---

\*[kbala@jpl.nasa.gov](mailto:kbala@jpl.nasa.gov); phone: 818-393-0258

## 2.1 Focal Plane Masks

**Gray Scale Masks:** Several kinds of focal plane masks have been fabricated and tested at JPL in recent years. Initially, band limited coronagraph masks with gray scale transmission profiles as shown in Figure 1 were designed and fabricated (Wilson, *et al.*, 2003)<sup>6</sup> at JPL with high energy electron beam sensitive (HEBS)<sup>7</sup> glass (Canyon Materials) which darkens to different optical density levels depending on the electron beam dose. However, such masks were found to suffer severely in broad band performance because of large wavelength dependent wavefront phase delay in transmission<sup>8,9</sup> due to the basic material properties of HEBS glass (Halverson, *et al.*, 2005, Balasubramanian, *et al.*, 2005). To overcome this problem, we examined the behavior of other materials and determined that gray scale metallic masks<sup>10,11</sup> could be designed and produced with chosen metals such as nickel, platinum, and Inconel (Balasubramanian, 2007). Therefore, Ni based masks (Figure 2) were fabricated at JPL by vacuum evaporation technique and tested in the high contrast imaging testbed (HCIT) reaching milestone results<sup>12</sup> (Trauger, *et al.*, 2007). Subsequently, dielectric over-coated metallic masks called “hybrid masks” have also been fabricated and tested<sup>13,14</sup> (Moody, *et al.*, 2008, Trauger, *et al.*, 2012).

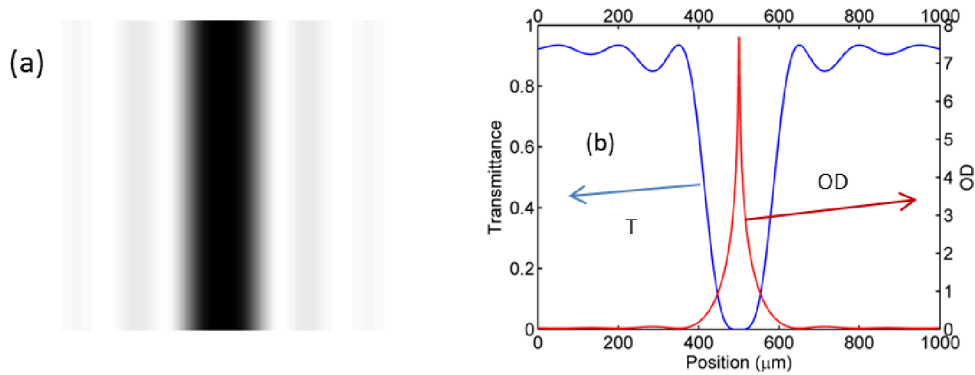


Figure 1. A typical 1-dimensional gray scale mask transmission image ((a) left) and cross- section transmittance and OD profiles ((b) right).

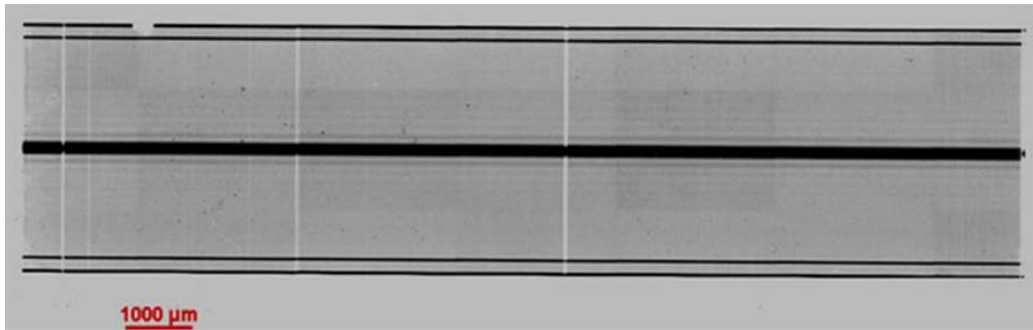


Figure 2. Transmission image of a focal plane mask fabricated with profiled Ni deposition on fused silica substrate

Metallic masks produced by vacuum deposition techniques tend to exhibit micron scale defects due to the process conditions and environment. Typical defects as shown in figure 3 lead to scatter levels of  $1e-7$  or brighter speckles. With linear masks whose spatial dependence is ideally one-dimensional, it is possible to search for a position where the level of defects is acceptable to achieve a high contrast in the coronagraph testbed. However, the centrally obscured circular apertures that are now available to NASA (the AFTA telescope) require circular masks. Circularly symmetric masks are also needed to improve the discovery space and thus the science benefits over the life of a coronagraph mission. With the starlight focused on the center of the mask, local defects on circularly symmetric masks could cause excessive scatter and poor performance. Fabricating circularly symmetric

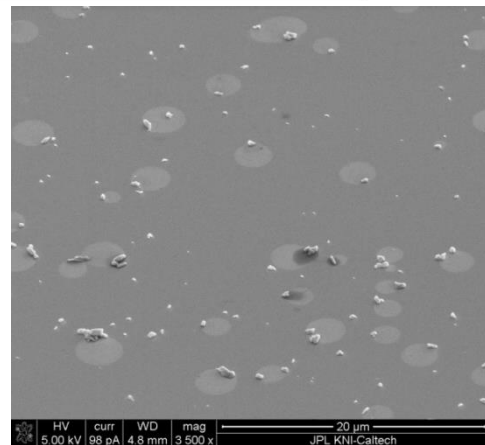


Figure 3. SEM image of a small region of metallic mask defects and contamination in high resolution

masks requires finer control of the processes to produce ideally defect-free masks with no contamination. New and improved techniques to fabricate circular masks are now under investigation.

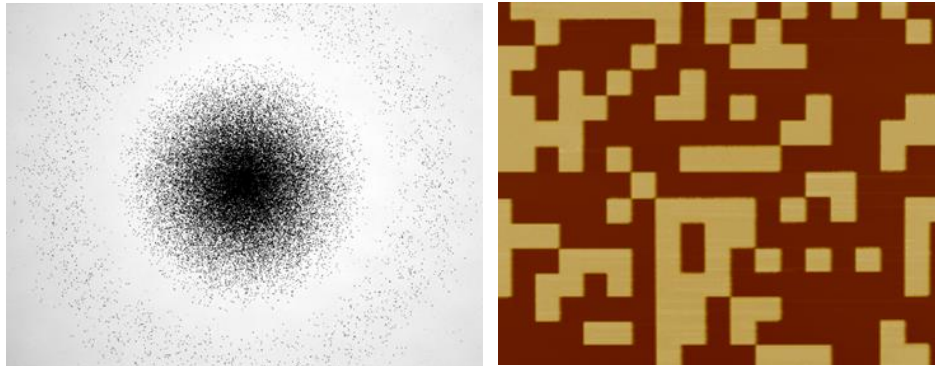


Figure 4. Micro dot patterned focal plane mask fabricated at JPL for JWST NIRCcam coronagraph  
Left: Macro image of the mask showing the inner core and a ring; Right: Micro dots in detail

#### Gray scale focal plane masks with binary micro dots

Employing electron beam lithography, the JPL team fabricated and delivered focal plane masks for JWST NIRCcam coronagraph system<sup>15</sup> with micro dots of aluminum on sapphire substrates as shown in Figure 4 to produce a gray scale mask to function in the near IR spectrum (Krist, *et al.*, 2010). Micro dot sizes and distribution are chosen based on model predictions considering optical interactions in wavelength scale features. These devices are currently being installed and integrated on NIRCcam at Lockheed Martin Space Systems Company in Palo Alto, CA.

#### Focal plane mask for Low Order Wavefront Sensor (LOWFS)

Another important mask that is needed for wavefront sensing in the coronagraph is an occulter to allow the light in the dark hole region to go to the science camera while reflecting the rest of the light to a sensing camera on another folded path. To accommodate the dynamic range of the camera, the brightest part of the psf is reflected significantly less (~ 0.1%) with an appropriately sized black silicon dot as shown in figure 5.

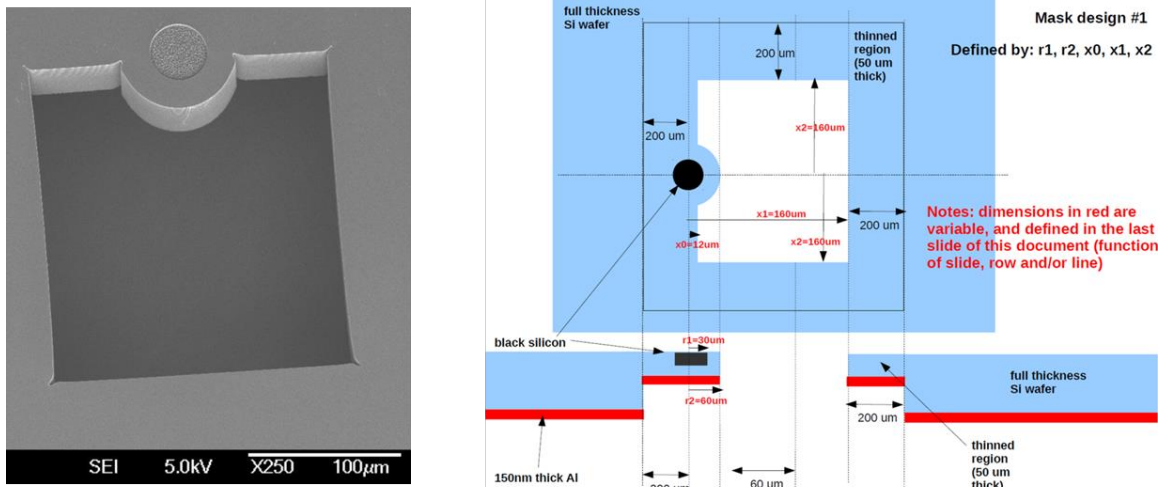


Figure 5. Low Order Wavefront Sensor (LOWFS)<sup>16</sup> mask on silicon with a black silicon dot at the image center. The light reflected off this occulter goes to the sensing camera. The punched hole region allows light in the dark hole to go to the science camera. Metallization of the backside ensures high optical density in the opaque regions.

Such a LOWFS mask has been employed in the PIAA testbed at JPL (Kern *et al.*, 2013)<sup>17</sup>. The mask was fabricated with a combination of lithographic patterning, deep reactive ion etching and a cryogenic etching process on silicon to produce the black dot.

### Achromatic Focal Plane Masks (AFPM) with diffractive structures

Another form of image plane mask is designed with diffractive structures as shown in figures 6 and 7; these masks scale with wavelength and hence behave as achromatic masks. Presently we produce these masks to serve in reflection because typical transmissive mask designs require deeper or taller structures, i.e.,  $>10\mu\text{m}$  which become less accurate due to electron scatter and thermal effects in the materials during e-beam exposure for lithography. Further process development is needed to control these effects. Diffractive structures designed to diffract light and scale with wavelength are aimed to function as achromatic masks (Newman, *et al.*, 2013)<sup>18,19</sup> in the focal plane of a coronagraph. The diffracted light is subsequently blocked by a Lyot stop so that a dark hole is created in the final image plane of the system. Such diffractive structures with about  $5\mu\text{m}$  depths/heights have been fabricated by grayscale electron beam lithography in e-beam polymer resist on silicon wafers. An example of pyramid like structures produced with a carefully optimized process is shown in figure 6. These masks were over-coated with aluminum and hence serve in reflective geometry with visible light. Tests with these masks in the testbed at NASA AMES Research Center showed the wavelength scaling characteristics as expected. More recently, transmissive AFPM masks were designed and fabricated in silicon (figure 7) for near IR spectrum and are now undergoing tests at the Subaru telescope adaptive optics laboratory.

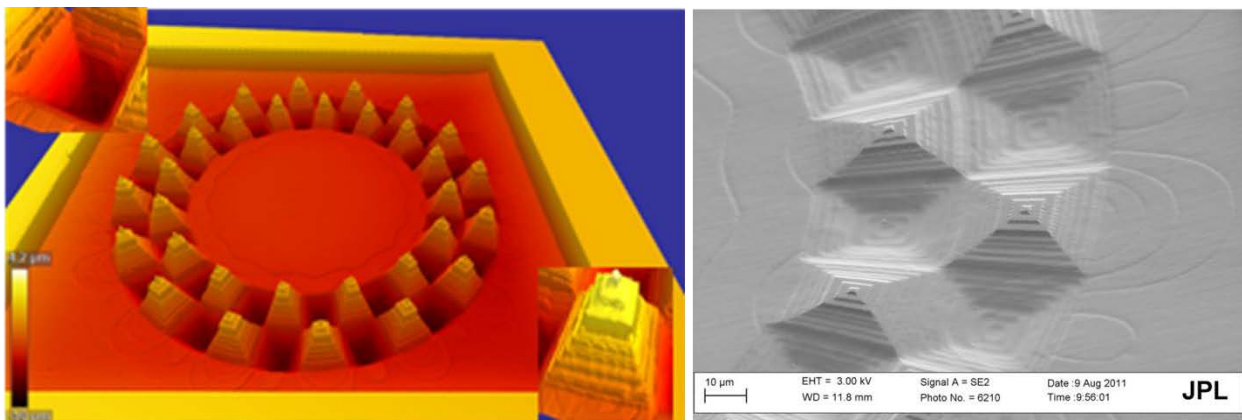


Figure 6. 3D image of pyramid structures fabricated for a reflective achromatic focal plane mask for AMES high contrast test bed

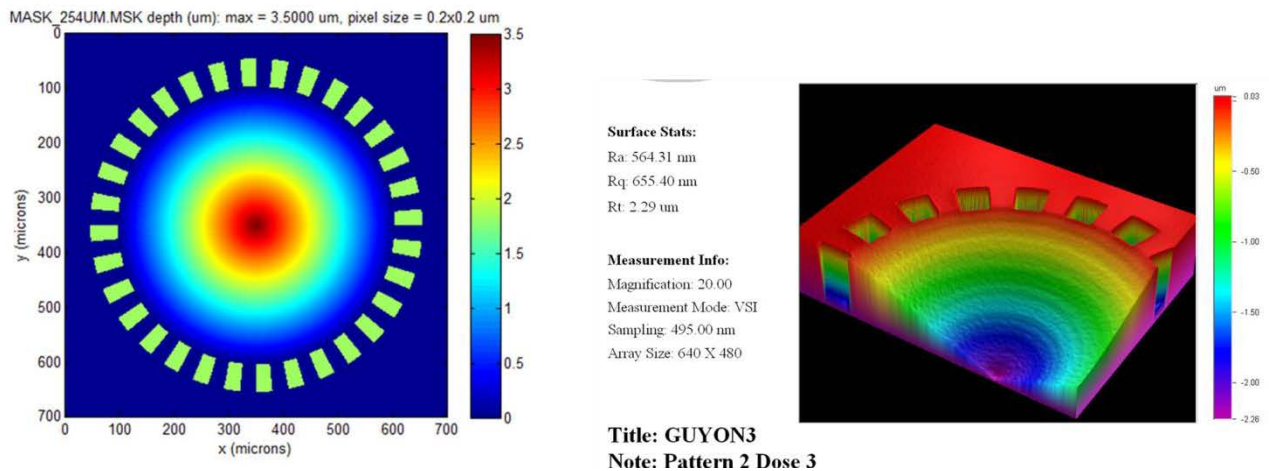


Figure 7. Achromatic focal plane mask (AFPM) designed to scale with wavelength in the near IR, and produced by grayscale e-beam lithography and plasma transfer etching into silicon at JPL. These silicon masks were made for tests at Subaru telescope adaptive optics laboratory for ground based observation of exoplanets.

## 2.2 Pupil Plane Masks

The concept of shaped pupil masks for coronagraphy has been studied extensively at Princeton University. Free-standing shaped pupil masks as designed by Princeton University team were fabricated by deep reactive ion etching (DRIE) technique at JPL. These masks shown in figure 8 were tested in the HCIT<sup>3,20</sup> (Belikov, *et al*, 2006, Balasubramanian, *et al*, 2006) at JPL. Pupil plane masks as shown in Figure 8 are binary approximations to continuous apodization functions. Rough walls of the slits in these masks produce excessive scattered light thus limiting the achievable coronagraph contrast. Shaping the walls with minimum thickness and roughness is a subject of current research and development at JPL.



Figure 8. Free-standing Shaped Pupil Masks designed for 25mm apertures (Princeton University designs); Fabricated at JPL for tests at Princeton labs and at JPL's High Contrast Imaging Testbed (HCIT). Clear white areas are open slits to transmit light. The SEM image on the right shows the rough inner walls of the slits.

More recent experiments with designing and producing shaped pupil masks particularly for tests at HCIT with 2 deformable mirrors are detailed in another presentation at this conference<sup>21</sup>. A microscope image of a mask with dithered whiskers fabricated for this experiment is shown in figure 9. The typical cross section of these slits fabricated on SOI (silicon on insulator) wafers is shown in figure 10.

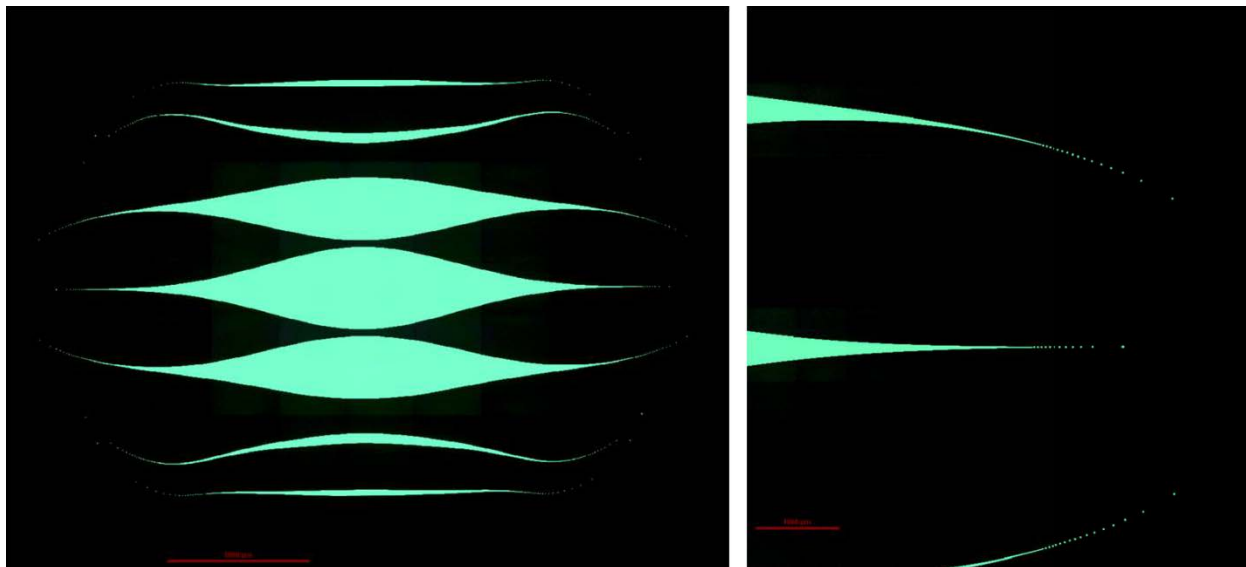
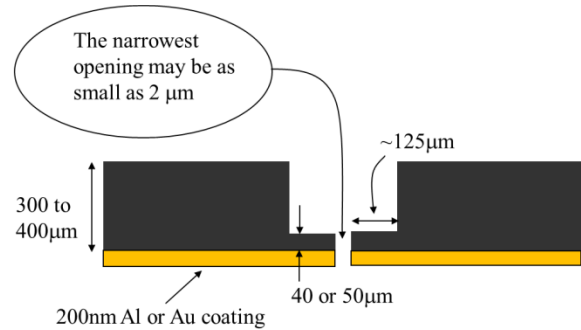


Figure 9 (a) Transmission image of a free-standing shaped pupil mask designed by Princeton and fabricated at JPL for 30mm dia HCIT pupil; sp 6-5-1 5x 0.15NA objective

(b) Image of the dithered edges of sp 6-5-1 20x 0.45NA objective

Figure 10. Typical cross section of slit or aperture with recessed step thus thinning the edge thickness to reduce optical scatter due to grazing incidence, surface plasmons and polarization effects. Free standing masks with silicon substrate as fabricated with such cross sections of various shapes as shown in figure 9.



### Patterned black silicon pupil mask

An alternative is to create reflective masks where the dark areas are made of ultra-low reflectivity black silicon on a silicon wafer. A reflective pupil apodizer can be manufactured with an etching process to produce micro structures on a silicon wafer patterned with e-beam lithography. A cryogenic “black silicon” process has been developed at JPL to produce various optical devices with black silicon structures, primarily to reduce stray light from slits and component surfaces. An Oxford System 100 Cryo ICP system available at Caltech Kavli Nanoscience Institute (KNI) is used to perform this highly anisotropic etch at cryogenic temperatures with appropriate gas chemistry. Needle-like structures with a few microns in diameter and tens of microns tall form a fine grass-like surface causing absorption of light within the silicon surface. Figure 11 shows the microstructure of such a black silicon surface. Typical reflection from these black silicon structures is ~0.1 to 1% in the visible spectrum. The specular reflectance depends on the microstructure and can be tailored with process conditions. Figure 12 shows the image of a black silicon based apodizer sample fabricated by the JPL team per Princeton University design. This device is currently undergoing tests at Princeton University. Application of these structures on a highly reflective substrate such as aluminum coated silicon wafer is a focus area for further development.

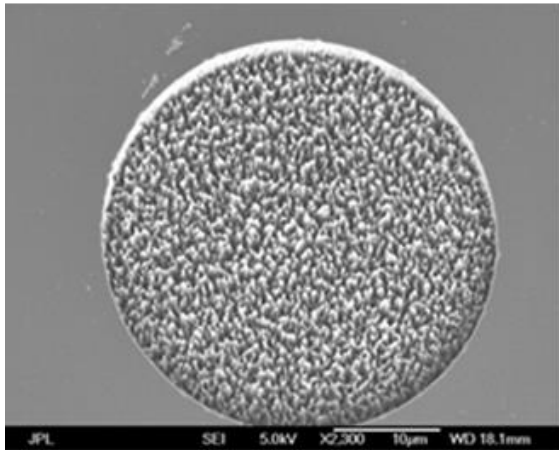
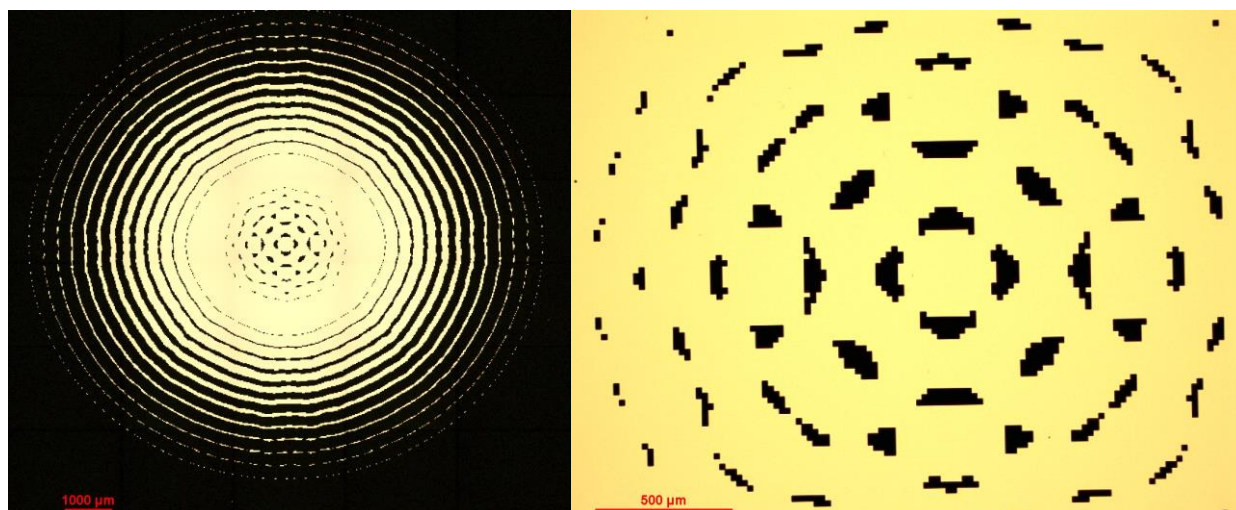


Figure 11 (left). SEM image of the microstructure of absorbing black silicon dot with typical reflectivity ~0.1 to 1% in the visible

Figure 12 (below). Patterned black silicon pupil mask: Optical microscope image of a pupil apodizer silicon sample; the black rings and structures are produced with cryogenic black silicon process. Left below: the full device; Right below: detail of the central region of the mask.



### Laboratory-scale external occulter type masks

Figure 12 shows views of a mask fabricated by deep reactive ion etching as part of an experiment to model the diffraction from a starshade in a subscale system. The shape of the inner section was chosen to mimic the effect of an external occulter, taking a design optimized for space, and scaling it down to be consistent with the size of the system. The shape of the outer section was selected to minimize the diffracted light from the outer ring across the entire occulter shadow. The minimum feature size was limited to 10 microns at the very tips of the holes; one can be seen on the right side of the figure. The detail of one petal on the mask in the right most figure shows the ledge on the edges of the recessed of petals as depicted in the cross section cartoon in figure 10. For more details on the design process, including the scaling and experimental results<sup>22</sup>, see Cady et al. 2009.

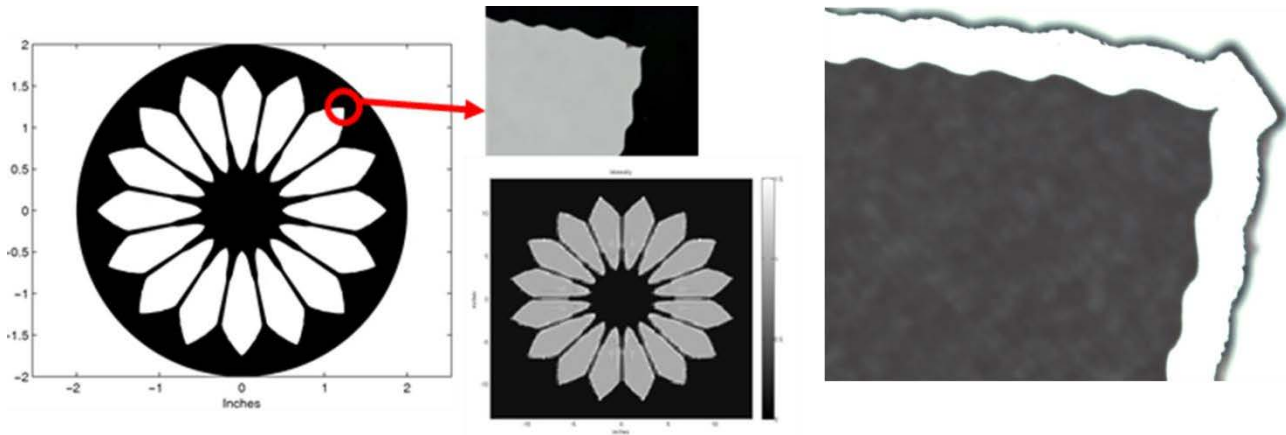


Figure 12. Lab scale external occulter type masks fabricated by deep reactive ion etching on SOI wafer. Princeton designed mask was produced at JPL for tests on Princeton high contrast lab.

### 2.3 Focused ion beam patterning of mask features

The Focused Ion Beam (FIB) technique is typically employed for repairs and failure analysis of microcircuits and for fabrication of metallic nanostructures. The semiconductor industry employs FIB instruments manufactured and sold by the FEI Company and Hitachi. Modern FIB instruments are equipped with a focused ion beam column as well as a scanning electron microscope (SEM) column to perform complementary functions of etching/deposition as well as imaging immediately after the process.

Caltech's Kavli Nanoscience Institute (KNI) operates an FIB instrument<sup>23</sup> from the FEI Company. This NOVA 600 tool is incorporated with both FIB and SEM columns with several gas inlets to deposit metals such as Pt and W. Deposition of some dielectrics is also conceivable with the FIB process.

Figure 13 shows a few marks of Pt deposited on chosen locations on a previously fabricated Ni gray scale focal plane mask; these marks serve as "calibrated defects" to measure contrast on HCIT to validate model predictions (Sidick et al., 2013)<sup>24</sup>. Figure 14 shows a few simple preliminary structures of Pt that we deposited on a thin Ni coated glass substrate. These structures demonstrate the feasibility to produce fine features of Pt and show the need for further development. The accuracy of feature sizes, proximity effects, defects, and optical properties of the device will be primary metrics to measure, evaluate and optimize. As the FIB process deposits material at 15 to 20 nm size spots and scans to fill a larger area, it allows fine controls while taking relatively long deposition time raising concerns of stability. The parameter space of ion beam energy, ion current, dwell time, over laps, scan sequence, etc., are the technical details to be optimized. But, FIB deposition is a significantly cleaner process than conventional vacuum deposition. Also, the dual beam system allows observation of the features and defects immediately after deposition without opening the chamber. Such a process, while still not mature, has the potential to fabricate circularly symmetric gray scale masks with chosen features at specific locations.

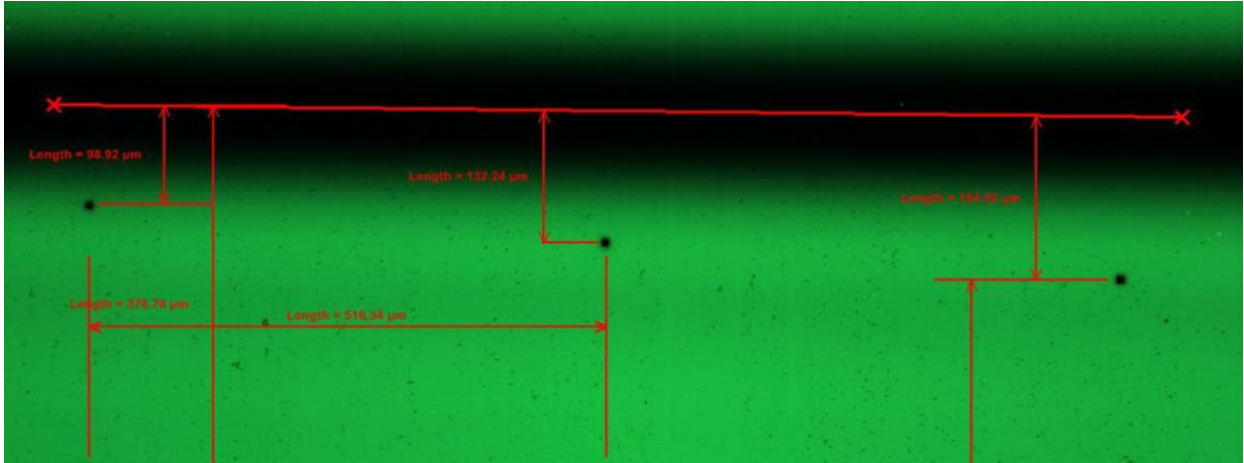


Figure 13. 6μm x 6μm Pt marks written by Focused Ion Beam technique at chosen locations on a previously fabricated metallic mask for model validation experiments on HCIT

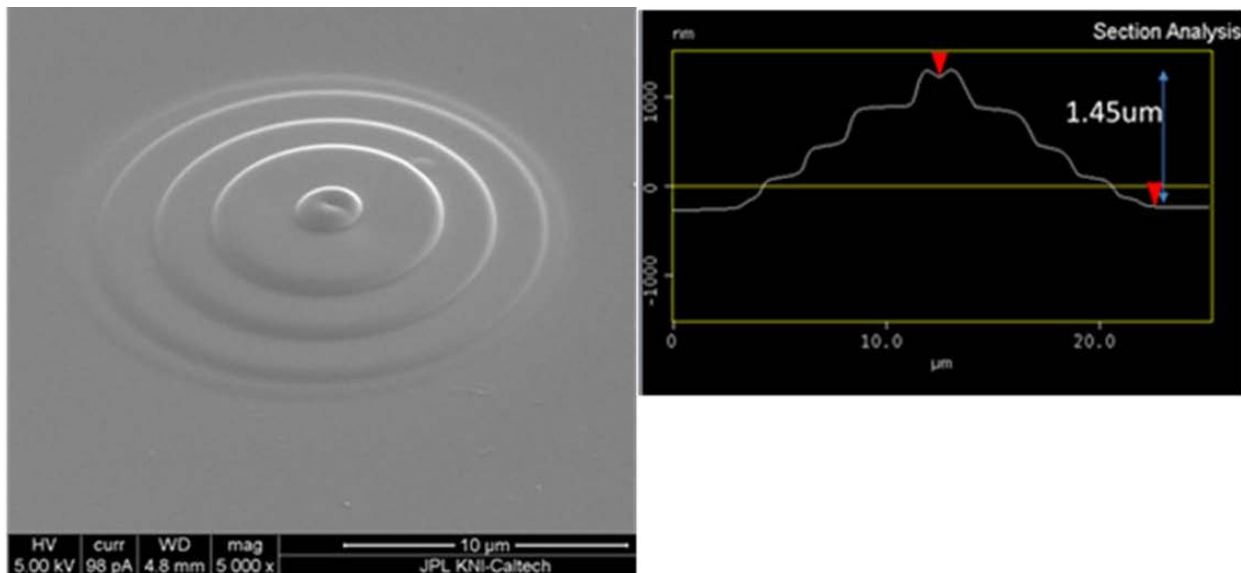


Figure 14. A pattern of stacked Pt discs of various diameters and thicknesses deposited on fused silica substrate by Focused Ion Beam technique, a potential method to fabricate circularly symmetric gray scale focal plane masks. Left: SEM image of stacked Pt discs, Right: AFM measurement of the stacked circular pattern

### 3. SUMMARY & CONCLUSIONS

Various types of masks and apodizers are needed for exoplanet coronagraph systems. Several techniques including physical vapor deposition, electron beam lithography, deep reactive ion etching, cryogenic etching of black silicon, focused ion beam deposition have been employed to produce various masks to serve in the focal plane as well as pupil plane. Illustrative examples of the different types of masks and their characteristics suggest a pathway with complimentary techniques to produce the more challenging circularly symmetric masks for coronagraph architectures for the AFTA telescope with an obscured pupil.

### 4. ACKNOWLEDGMENTS

This work was performed at the Jet Propulsion Laboratory, California Institute of Technology, under a contract with the National Aeronautics and Space Administration.

## REFERENCES

- [1] Trauger, *et al.*, J. T. Coronagraph contrast demonstrations with the High Contrast Imaging Testbed, Proc. SPIE, Vol. 5487, pp. 1330-1336, (2004).
- [2] Trauger, J. T. and W.A. Traub, "A laboratory demonstration of the capability to image an Earth-like extrasolar planet", Nature, Vol.446, pp. 771-773. (2007).
- [3] Belikov, R., *et al.*, "Towards  $10^{-10}$  Contrast for Terrestrial Exoplanet Detection: Demonstration of Extreme Wavefront Correction in a Shaped-Pupil Coronagraph", Proc. SPIE vol.6265-42, (2006)
- [4] Mawet, D. *et al.*, "Taking the vector vortex coronagraph to the next level for ground- and space-based exoplanet imaging instruments: review of technology developments in the USA, Japan, and Europe", Techniques and Instrumentation for Detection of Exoplanets V, ed: Stuart Shaklan, Proc. of SPIE Vol. 8151, (2011)
- [5] Guyon, O. "Exoplanet Imaging with a Phase-induced Amplitude Apodization Coronagraph. I. Principle" . *Astrophysical Journal ApJ* 622 , 744. (2005).
- [6] Wilson, D.W., P. D. Maker, J.T. Trauger, T.B. Hull. "Eclipse apodization: realization of occulting spots and Lyot masks," Proc. SPIE, Vol. 4860, 361-370, 2003.
- [7] Canyon Materials, Inc. San Diego CA, USA. <http://canyonmaterials.com>
- [8] Halverson, P. G. *et al.*, "Measurement of phase and optical density of TPF coronagraph occulting mask materials", in Techniques and Instrumentation for Detection of Exoplanets II, edited by Daniel R. Coulter, Proc. Vol., SPIE **5905**, 11-10, (2005).
- [9] Balasubramanian, K., *et al.*, "Occulting Focal Plane Masks for Terrestrial Planet Finder Coronagraph: Design, Fabrication, Simulations and Test Results" Proc. of IAU Colloquium No. 200, 2005, Direct Imaging of Exoplanets, C. Aime and F. Vakili, Eds., Nice, France Oct (2005).
- [10] Balasubramanian, K., *et al.*, "Band-limited masks for TPF coronagraph", C. R. Physique 8, vol. 8, Issue 3-4, p. 288-297, (2007).
- [11] Balasubramanian, K., "Band-limited image plane masks for the Terrestrial Planet Finder coronagraph: materials and designs for broadband performance", Appl. Optics, Vol. 47, No. 2, 116-125, (2008).
- [12] Trauger, J. T. and W.A. Traub, "A laboratory demonstration of the capability to image an Earth-like extrasolar planet", Nature, Vol.446, pp. 771-773. (2007).
- [13] Moody, D.C., B.L. Gordon, J.T. Trauger, "Design and demonstration of hybrid Lyot coronagraph masks for improved spectral bandwidth and throughput", Proc. of SPIE Vol. 7010, 70103P, (2008)
- [14] Trauger, J., *et al.*, "Complex apodization Lyot coronagraphy for the direct imaging of exoplanet systems: design, fabrication, and laboratory demonstration", Proc. SPIE Vol. 8442 (2012)
- [15] Krist, John E., *et al.*, "The JWST/NIRCam coronagraph flight occulters" , in Space Telescopes and Instrumentation 2010: Optical, Infrared, and Millimeter Wave, Proc. SPIE Vol. 7731, (2010)
- [16] Guyon, O., Taro Matsuo, Roger Angel, "Coronagraphic Low Order Wavefront Sensor: Principle and Application to a Phase-Induced Amplitude Coronagraph", ApJ, 693, pp 75-84 (2009)
- [17] Kern, B., *et al.*, "Laboratory demonstration of Phase Induced Amplitude Apodization (PIAA) coronagraph with better than  $10^{-9}$  contrast", presented in Optics & Photonics SPIE 2013; also, NASA ROSES TDEM PIAA Milestone 1 Report (2013)
- [18] Newman, K., R. Belikov, O. Guyon, K. Balasubramanian, D. Wilson, E. Pluzhnik, "Achromatic Focal Plane Mask for Exoplanet Imaging Coronagraphy", 221<sup>st</sup> meeting of the American Astronomical Society, Long Beach, CA, Jan. 6-10, 2013
- [19] Newman, K., *et al.*, "Achromatic focal plane mask for exoplanet imaging coronagraphy", Proc. SPIE Vol. 8864-51, (2013)
- [20] Balasubramanian, K., *et al.*, "Fabrication and Characteristics of Free Standing Shaped Pupil Masks for TPF Coronagraph," Proc. of SPIE, 6265 (2006).
- [21] Riggs, A.J.E., *et al.*, "Demonstration of symmetric dark holes using two deformable mirrors at the high-contrast imaging testbed", Proc. SPIE Vol. 8864-28, (2013)
- [22] Cady, E., *et al.*, "Progress on the occulter experiment at Princeton", Proc SPIE vol. 7440, (2009)
- [23] [http://www.fei.com/uploadedfiles/documentsprivate/content/2006\\_06\\_nova600nanolab\\_pb.pdf](http://www.fei.com/uploadedfiles/documentsprivate/content/2006_06_nova600nanolab_pb.pdf)
- [24] Sidick, E. *et al.*, HCIT Contrast Performance Sensitivity Studies: Simulation versus Experiment, Proc. SPIE vol. 8864 (2013)